Analysis of Regular and Chaotic Dynamics of the Euler-Bernoulli Beams Using Finite-Difference and Finite-Element Methods

Anton Krysko, Jan Awrejcewicz, Maxim Zhigalov, and Olga Saltykowa

1 Introduction

Owing to remarkable development of aeronautics, astronautics and ship-building industry, the problem of an accurate and engineering-accepted beam dynamics (taking into account various boundary conditions and sign changeable loads) is of high importance. It is well known that the problems yielded by mechanical engineering require construction and analysis of their mathematical models. Modeling of flexible beam vibrations subjected to transversal and longitudinal sign-changeable loads belongs to one of the hottest problems of today's mechanics. Key targets of modeling and analysis of beams, plates and shells include studies of transition from regular to chaotic dynamics and vice versa, and the methods of dynamics control via external load action (see, for instance, references [1–5]).

Our aim in this work was to compare results of two different methods of mathematical modeling, i.e. FDM and FEM, using the example of Euler-Bernoulli type flexible beams.

2 Problem Formulation

A mathematical model of transversal Euler-Bernoulli beam vibrations with various boundary conditions is derived in this work. The Cartesian coordinates system XOZ is introduced, and then in the space $\Omega = \left\{x \in [0,a]; -h \le z \le h; -\frac{b}{2} \le y \le \frac{b}{2}\right\}$ a thin

A. Krysko
The Saratov State Technical University, Department of Applied Mathematics, Saratov, Russia,
e-mail: tak@san.ru

J. Awrejcewicz
Technical University of Lodz, Department of Automatics and Biomechanics, Lodz, Poland,
e-mail: awrejcew@p.lodz.pl

M. Zhigalov and O. Saltykowa
The Saratov State Technical University, Department of Higher Mathematics, Saratov, Russia,
e-mail: ZhigalovM@yandex.ru, olga_saltykova@mail.ru.

J. Awrejcewicz (ed.) *Modeling, Simulation and Control of Nonlinear Engineering Dynamical Systems.*

elastic beam with its middle surface deformation $\varepsilon_x = \frac{\partial u}{\partial x} + \frac{1}{2}\left(\frac{\partial w}{\partial x}\right)^2$ is studied, where $w(x,t)$ denotes beam deflection, and $u(x,t)$ is the middle surface displacement along the ox axis. It is assumed that owing to the Euler-Bernoulli hypothesis a normal to the beam middle surface is still normal after the beam deformation: $\varepsilon_{xx} = \varepsilon_x - z\frac{\partial^2 w}{\partial x^2}$, where ε_x is the middle surface deformation, $N_x = \int\limits_{-h}^{h} \sigma_{xx} dz$ is the longitudinal force, and $M_x = \int\limits_{-h}^{h} \sigma_{xx} z dz = -\frac{(2h)^3}{12} E \frac{\partial^2 w}{\partial x^2}$ denotes the bending moment. Dynamics governing equations have the following form [6]:

$$\begin{cases} E(2h)\left\{\frac{\partial^2 u}{\partial x^2} + L_3(w,w)\right\} - (2h)\frac{\gamma}{g}\frac{\partial^2 u}{\partial t^2} - \varepsilon_2(2h)\frac{\gamma}{g}\frac{\partial u}{\partial t} = 0, \\ E(2h)\left\{L_1(u,w) + L_2(w,w) - \frac{(2h)^2}{12}\frac{\partial^4 w}{\partial x^4}\right\} + q - (2h)\frac{\gamma}{g}\frac{\partial^2 w}{\partial t^2} - \varepsilon_1(2h)\frac{\gamma}{g}\frac{\partial w}{\partial t} = 0, \end{cases} \tag{1}$$

where $L_1(u,w) = \frac{\partial^2 u}{\partial x^2}\frac{\partial w}{\partial x} + \frac{\partial u}{\partial x}\frac{\partial^2 w}{\partial x^2}$, $L_2(w,w) = \frac{3}{2}\frac{\partial^2 w}{\partial x^2}\left(\frac{\partial w}{\partial x}\right)^2$, $L_3(w,w) = \frac{\partial^2 w}{\partial x^2}\frac{\partial w}{\partial x}$, ε_1, ε_2 – dissipation coefficients; $q = q(x,t)$ – transversal load, E – Young modulus, ρ, γ – density and weight density, respectively, and g – acceleration of gravity. The following non-dimensional variables are introduced

$$\begin{gathered} \bar{w} = \frac{w}{(2h)},\ \bar{u} = \frac{ua}{(2h)^2},\ \bar{x} = \frac{x}{a},\ \lambda = \frac{a}{(2h)},\ \bar{q} = q\frac{a^4}{(2h)^4 E}, \\ \bar{t} = \frac{t}{\tau},\ \tau = \frac{a}{c},\ c = \sqrt{\frac{Eg}{\gamma}},\ \bar{\varepsilon}_i = \varepsilon_i \frac{a}{c}, i = 1,2. \end{gathered} \tag{2}$$

Taking into account (2), system (1) takes the form

$$\begin{cases} \frac{\partial^2 u}{\partial x^2} + L_3(w,w) - \frac{\partial^2 u}{\partial t^2} - \varepsilon_2\frac{\partial u}{\partial t} = 0, \\ \frac{1}{\lambda^2}\left\{L_2(w,w) + L_1(u,w) - \frac{1}{12}\frac{\partial^4 w}{\partial x^4}\right\} - \frac{\partial^2 w}{\partial t^2} - \varepsilon_1\frac{\partial w}{\partial t} + q = 0, \end{cases} \tag{3}$$

where in the above bars over non-dimensional quantities are omitted.

The following boundary conditions at the beam ends are attached to Eqs. (3):

Problem 1. "Clamping – clamping":

$$w(0,t) = w(a,t) = u(0,t) = u(a,t) = \frac{\partial w(0,t)}{\partial x} = \frac{\partial w(a,t)}{\partial x} = 0. \tag{4}$$

Problem 2. "Hinge – hinge":

$$w(0,t) = w(a,t) = u(0,t) = u(a,t) = 0; M_x(0,t) = M_x(a,t) = 0. \tag{5}$$

Problem 3. "Hinge – clamping":

$$w(0,t) = w(a,t) = u(0,t) = u(a,t) = 0; M_x(0,t) = 0; \frac{\partial w(a,t)}{\partial x} = 0. \quad (6)$$

Problem 4. "Hinge – free":

$$w(0,t) = M_x(0,t) = u(0,t) = 0; M_x(a,t) = N_x(a,t) = Q_x(a,t) = 0. \quad (7)$$

Additionally, the following initial conditions are attached to Eqs. (3) through (7):

$$w(x,t)_{|t=0} = \left.\frac{\partial w(x,t)}{\partial t}\right|_{t=0} = u(x,t)_{|t=0} = \left.\frac{\partial u(x,t)}{\partial t}\right|_{t=0} = 0. \quad (8)$$

3 On the Numerical Solution to Vibration and Stability Beam Problems

Investigation of nonlinear vibrations of constructions with various dynamic states (regular and/or chaotic) requires highly accurate computational algorithms and implementation of numerical methods. Since analytical methods devoted to the analysis of non-linear models can be rarely applied, the only way is to apply various numerical approaches to verification of reliability of the obtained results. In this work, various numerical approaches are applied, namely direct one (FDM) and variational one (FEM) in the Bubnov-Galerkin form. A comparison is made for various boundary conditions and for various dynamic regimes. In all investigated cases the beam geometric and physical parameters are taken as the same.

3.1 FDM with Approximation $O(c^2)$

The infinite dimensional problem (3)–(8) can be reduced to the finite dimensional one via the finite difference method (FDM) with approximation $O(c^2)$. Namely, at each mesh node the following system of ordinary differential equations is obtained:

$$\begin{aligned} &L_{1,c}(w_i,u_i) = \varepsilon_1 \dot{w}_i + \ddot{w}_i, \\ &L_{2,c}(w_i,u_i) = \varepsilon_2 \dot{u}_i + \ddot{u}_i, \\ &(i = 0,\ldots,n), \end{aligned} \quad (9)$$

where n denotes the partition numbers regarding spatial coordinates, and

$$L_{2.c}(w_i,u_i)=\frac{1}{c^2}(u_{i+1}-2u_i+u_{i-1})+\frac{1}{2c}(w_{i-1}-w_{i+1})\frac{1}{c^2}(w_{i+1}-2w_i+w_{i-1}),$$

$$L_{1.c}(w_i,u_i)=\frac{1}{\lambda^2}(-\frac{1}{12}\frac{1}{c^4}(w_{i-2}-4w_{i-1}+6w_i-4w_{i+1}+w_{i+2})+$$

$$+\frac{1}{2c}(w_{i-1}-w_{i+1})\frac{1}{c^2}(u_{i+1}-2u_i+u_{i-1})+\frac{1}{2c}(w_{i-1}-w_{i+1})\frac{1}{c^2}(u_{i+1}-2u_i+u_{i-1})+$$

$$+\left(\frac{1}{2c}(w_{i-1}-w_{i+1})\right)^2\frac{1}{c^2}(w_{i+1}-2w_i+w_{i-1})+$$

$$+\frac{1}{c^2}(w_{i+1}-2w_i+w_{i-1})\left(\frac{1}{2c}(u_{i+1}-u_{i-1})+\frac{1}{8c^2}(w_{i-1}-w_{i+1})(w_{i-1}-w_{i+1})\right)+q).$$

For $i=1$, $i=n-1$ one has to take into consideration the so-called out of contour points, which are defined by the following boundary conditions: for problem 1 $w_{-i}=w_i$, whereas for problem 2 $w_{-i}=-w_i$. The following additional equations are supplemented to Eqs. (9) for

Problems 1–3:

$$w_0=0;\quad w_n=0;\quad u_0=0;\quad u_n=0, \tag{10}$$

and for Problem 4

$$w_0=0;\quad u_0=0;\quad M_x=0;\quad N_x=0;\quad Q_x=0. \tag{11}$$

The initial conditions (8) for the considered cases have the following difference form

$$w(x_i)_{|t=0}=0;\ u(x_i)_{|t=0}=0;\ \dot{w}(x_i)_{|t=0}=0;\ \dot{u}(x_i)_{|t=0}=0,\ i=0,\ldots,n. \tag{12}$$

3.2 FEM with the Bubnov-Galerkin Approximation

The so far defined problem (3)–(8) is solved now via FEM. Owing to the FEM theory, in order to construct a beam element we need to introduce the testing functions. The following four degrees of freedom (w_1, w_2, θ_1, θ_2) are associated with the element and the following approximation polynomial is applied:

$$w(x)=a_1+a_2x+a_3x^2+a_4x^3,\theta(x)=-\frac{dw}{dx}=-\left(a_2+2a_3x+3a_4x^2\right).$$

After defining the constant values, an approximation function has the following form:

$$w=\lfloor \mathbf{N}_w \rfloor \{\mathbf{W}\}$$

where $[\mathbf{N}_w]=\left(1-3\xi^2+2\varsigma^3;-l\xi(\xi-1)^2;3\xi^2-2\xi^3;-l\xi\left(\xi^2-\xi\right)\right)$ – form matrix; $\{\mathbf{W}\}=(w_1,\ \theta_1,\ w_2,\ \theta_2)^{\mathrm{T}}$ – node displacement matrix; $\xi=x/l$ – non-dimensional quantity (local coordinate).

Displacement approximation $u(x)$ has the following form:

$$u = \lfloor \mathbf{N}_u \rfloor \{\mathbf{U}\},$$

where $\lfloor \mathbf{N}_u \rfloor = (1-\xi;\xi)\{\mathbf{U}\} = (u_1 \quad u_2)^{\mathrm{T}}$.

Applying the Bubnov-Galerkin procedure and taking into account the introduced approximations, the following equations of FEM are obtained

$$\begin{cases} M_1 [\ddot{W}] + C_1 [\dot{W}] + K_1 [W] = F_1 (q, U), \\ M_2 [\ddot{U}] + C_2 [\dot{U}] + K_2 [U] = F_2 (p, W), \end{cases} \tag{13}$$

where M_i, C_i, K_i are the matrices of mass, damping and stiffness, respectively.

4 Numerical Results Obtained via FDM and FEM

The considered beam is subjected to the action of the following transversal load

$$q = q_0 \sin(\omega_p t), \tag{14}$$

where ω_p is the excitation frequency, and q_0 is its amplitude. The studied system is dissipative, and the damping coefficients denoted by ε_1, ε_2 correspond to deflection w and displacement u, respectively.

Next, we study numerically the beam dynamics and stability. Any method of beam partition allows us to approximate PDEs by ODEs. Integration of the latter ones can be divided into two groups, i.e. explicit and implicit methods. The explicit methods are mainly realized via the Runge-Kutta schemes, and they are sufficient to solve our beam problem. It is mainly motivated by an observation that the considered Cauchy problem does not belong to stiff one, since in the frequency spectrum of eigen values of the Bernoulli-Euler type equations there are no frequencies differing in the order of magnitude (see, for instance, considerations in reference [7]).

In order to verify the validity and accuracy of beam vibration simulations, both mentioned methods (FEM and FDM) are applied in problem 4, and the following fixed damping coefficients $\varepsilon_1 = 1$, $\varepsilon_2 = 0$, where $\omega_p = 5.1$ is the excitation frequency, and $\lambda = a/2h = 50$ denotes the relative beam length. The beam is subjected to the harmonic load action with the amplitude q_0. The computation step regarding spatial coordinate equals c and time step is Δt. Both of them are yielded by the Runge principle. The stated problem is solved for beam partitions $n = 40$, $c = 1/40$, and with the time step $\Delta t = 0.9052 \cdot 10^{-3}$. In order to compare the numerical results, power spectra and time histories (signals) $w(t)$are reported in Table 1 for $q_0 = 100$ (it corresponds to regular dynamics), and for $q_0 = 3{,}200$ (it corresponds to chaotic dynamics).

From Table 1 one may conclude that signals obtained via FEM and FDM practically coincide for the case of regular dynamics. In the case of chaotic dynamics, a

Table 1 Power spectra and time histories $w(t)$ for $q_0 = 100$ and for $q_0 = 3,200$

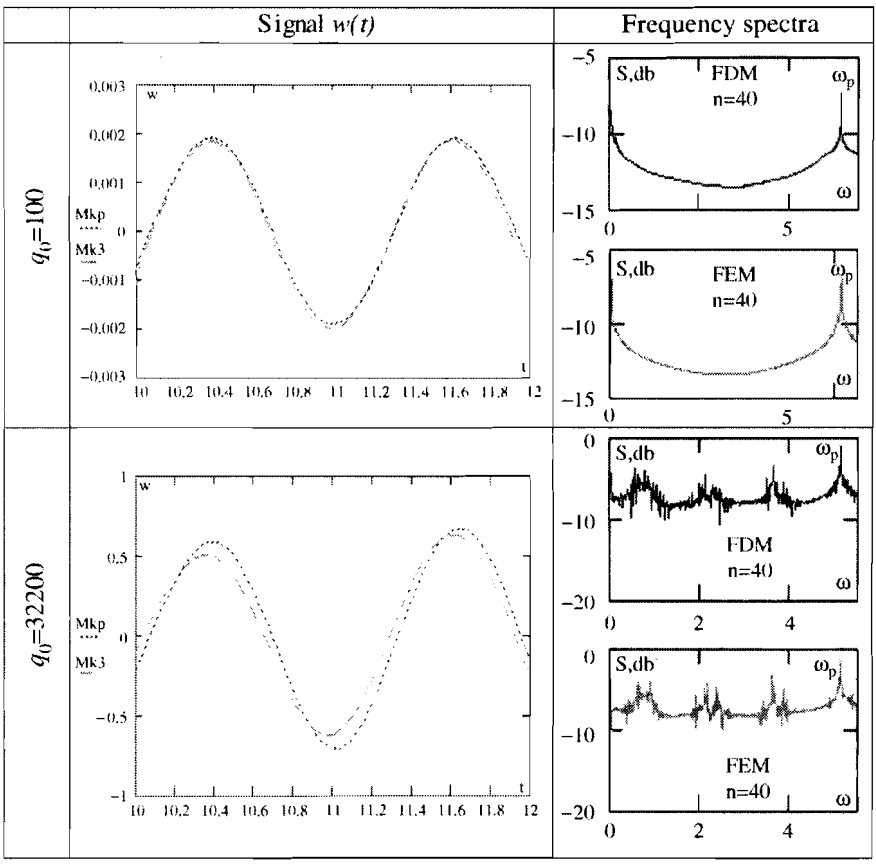

signal produced by FDM is slightly delayed in comparison to that produced by FEM and possesses smaller amplitude. Frequency power spectra of vibrations practically either coincide in the case of regular dynamics or are close to each other in the case of chaotic dynamics. Hence, owing to the results included in Table 1, the results obtained via the FEM and FDM methods are reliable for either regular or chaotic beam dynamics analysis.

In order to investigate beams dynamics driven by harmonic loads a special program package has been developed enabling construction of vibration type charts vs. control parameters $\{q_0, \omega_p\}$. For instance, in order to construct a chart with the resolution of 200 × 200 points, one needs to solve a problem of dynamics, to analyze frequency power spectrum and finally to compute the Lyapunov exponents for each choice of the control parameters. The developed algorithm enables also separation of the periodic dynamic zones, the Hopf bifurcation zones, quasi-periodic zones, as well as chaotic zones.

Table 2 Vibration type charts vs. Control parameters $\{q_0, \omega_p\}$ for problem 4

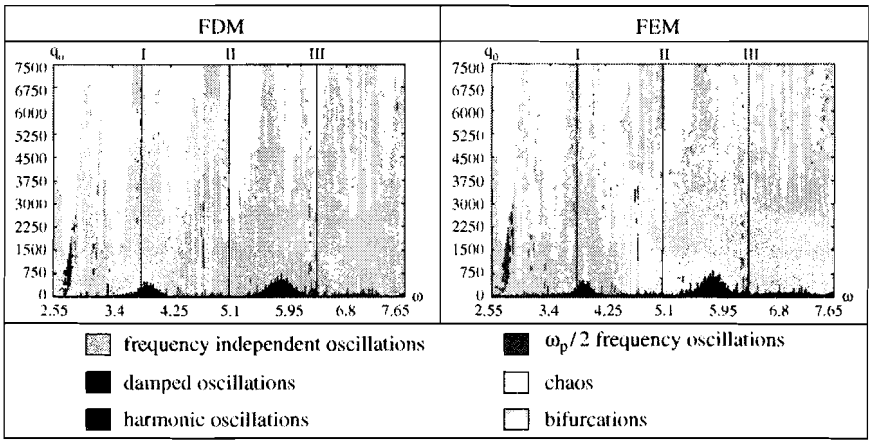

In Table 2, the vibration type charts vs. the control parameters $\{q_0, \omega_p\}$ for problem 4 are reported. Charts are constructed either with the application of FEM or FDM with the following fixed parameters $\varepsilon_1 = 0.1, \varepsilon_2 = 0$ for the beam length partition $n = 40$, and for the beam relative length $\lambda = a/2h = 50$. The excitation frequency changes from $\omega_0/2$ (chart I) to $3\omega_0/2$ (chart III), where ω_0 (chart II) denotes free frequency of the associated linear system (for problem 4 we have $\omega_0 = 5.1$). A maximal excitation amplitude corresponds to the beam deflection of $5(2h)$, and the charts are built with resolution 300×300.

Analysis of the obtained vibration type charts also supports reliability of the results obtained for various vibration regimes. Observe that the zones of chaotic vibrations vs. frequency obtained via FEM are wider than those obtained via FDM, whereas they coincide regarding the amplitude of vibrations. In order to get a vibration character chart vs. control parameters with resolution 300×300 one has to carry out 9·104 computational variants. In the case of FEM, the computational time increases about 1.5 times comparing to the FDM application (for n = 40). The notation introduced in Table 2, regarding vibration type, is also used further. Computation of such a chart with the use of a Celeron 1700 processor takes 400 days. However, the knowledge of such charts enables a full system control.

In order to confirm reliability of the results obtained for other types of boundary conditions, in Table 3 scales of vibration type beam character depending on the excitation amplitude $q_0 \in \lfloor 0.6 \times 10^4 \rfloor$ and for one value of ω_p are reported, and also dependences $w_{max}(q_0)$ are shown.

The problems are solved for the following parameters: $\varepsilon_1 = 1, \varepsilon_2 = 0, \lambda = a/2h = 50$, $\omega_p = 6.9$, and beam partition regarding spatial coordinate $n = 40$.

We show how the boundary conditions essentially influence the system dynamics. For Problem 1, the beam exhibits periodic and bifurcation type dynamics (either for FDM or for FEM). In this case there is no transition to chaotic dynamics. In graph $w_{max}(q_0)$ sudden jumps do not occur, and the function is smooth. In

Table 3 Beam vibrations depending on excitation amplitude $q_0 \in [0.6 * 10^4]$

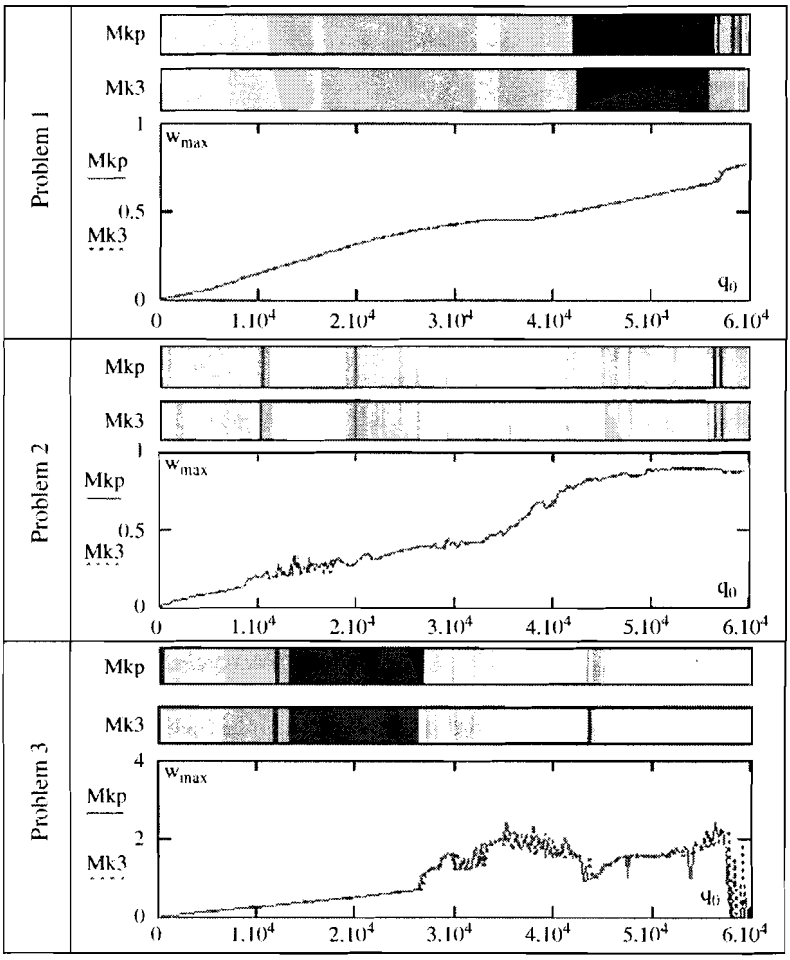

Problem 2, one may observe chaotic zones matched with bifurcation zones, but periodic dynamics is not exhibited. A function presenting maximal deflection vs. excitation amplitude is smooth only at the beginning (for $q_0 = 0.1 \cdot 10^4$), where sudden jumps of w_{max} are not observed. Transition of the system from periodic to chaotic vibrations and vice versa, is characterized by sudden changes of w_{max} even for a small change of the excitation amplitude, and this is understood as stability loss of the system dynamics.

In the case of non-symmetric boundary conditions (Problem 3) one may observe that the system transition into chaotic state occurs for $q_0 > 2.5 \cdot 10^4$. For the given boundary conditions periodic dynamics occurs for $q_0 \in (1.1, 2.5) \cdot 10^4$. It is remarkable that within beam chaotic regime in the graph $w_{max}(q_0)$ not only sudden jumps appear but also the functions are discontinuous.

5 Transition Scenarios into Chaos

As the earlier results of local chaos investigations show, there are a few typical transition scenarios leading a dynamic system from periodicity into chaos, which sometimes are also combined. On the other hand, as it will be shown further, such transitions, however, understood globally, may differ for the same system (here beam) for various boundary conditions. Mainly four typical transitions are well understood, namely the Landau-Hopf scenario, the Ruelle-Takens-Newhouse scenario, the Feigenbaum scenario and the Pomeau-Manneville scenario.

Below, we investigate and define a beam scenario of transition into chaos for Problem 2. The numerical investigation is carried out by two methods: FEM and FDM. Table 4 shows the fundamental steps helping in the scenario detection.

Observe that for $q_0 = 100$, in a frequency power spectrum, only frequency of excitation $\omega_p = 6.9$ is exhibited.

An increasing amplitude of excitation causes the occurrence of two independent frequencies (quasi-periodicity), which are evidenced by FEM and FDM, and their estimated values are the same. A further increase of the excitation amplitude causes the occurrence of linear combinations of the earlier mentioned frequencies $\omega_p, \omega_1, \omega_2$.

For example, let us study the system behavior for $q_0 = 11{,}000$ applying FDM. It is remarkable that the system dynamics is governed by a linear combination of frequencies $\omega_p, \omega_2, \omega_4$. The following three frequency groups are distinguished: $\omega_4, \omega_7, \omega_9$ – the first group, where frequency values differ by the amount of frequency ω_4; $\omega_1, \omega_2, \omega_{10}, \omega_{11}$ – the second group, where the frequencies differ from each other either by ω_4, or by $\omega_4 \cdot 2$; $\omega_p, \omega_3, \omega_5, \omega_8$ – the third group, where the linear combination of frequencies is preserved. Observe that an analogous system behavior is also monitored for $q_0 = 8{,}700$ in the case of FEM application.

A further increase of q_0 yields more evident changes of the earlier mentioned frequencies, and finally all of the frequencies become linearly dependent. For $q_0 = 20{,}000$ (FDM) and for $q_0 = 19{,}900$ (FEM) all frequency distances are almost equal, and the difference between them achieves 1.062.

6 Conclusions

An increase of the amplitude of external excitation causes variation of frequencies. The mentioned frequencies again appear and disappear. As a result, in the frequency spectra, either for FDM or for FEM, one may distinguish six linearly independent groups of frequencies, each group containing linearly dependent frequencies which differ by the amount of 0.29. Then, when all of the born frequencies become linearly dependent, the system dynamics is transited into chaotic state, which is clearly manifested by the system frequency spectra for $q_0 = 4 \cdot 10^4$ (FDM) and $q_0 = 4.9 \cdot 10^4$ (FEM).

Table 4 Some fundamental steps helping in the scenario detection

	q_0	Power spectrum $S(\omega_p)$	Signal $w(05, t)$	Phase portrait $w(\dot{w}\&)$
FDM	100	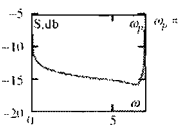	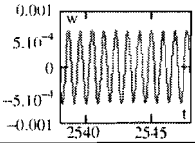	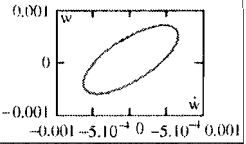
FEM	100	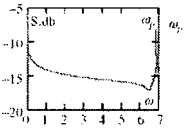	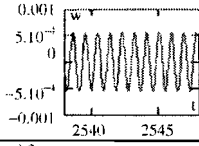	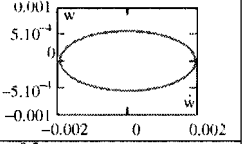
FDM	11000	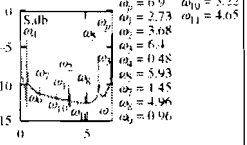	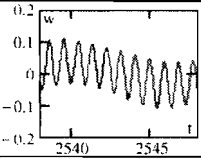	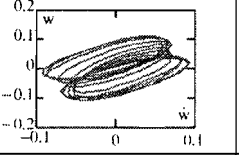
FEM	8700	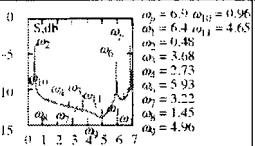	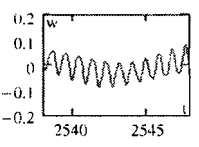	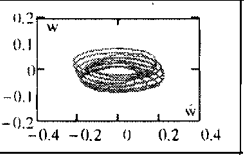
FDM	20000	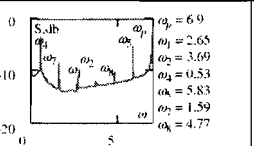	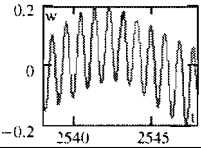	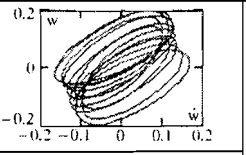
FEM	19900	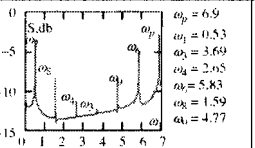	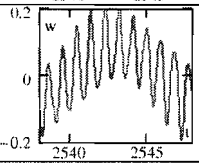	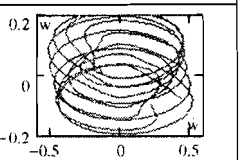
FDM	40000	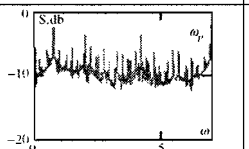	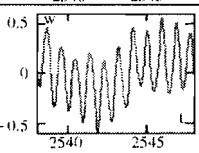	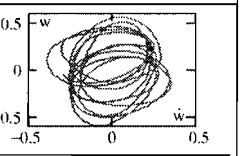
FEM	39900	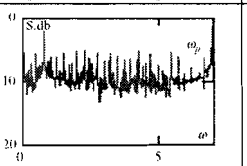	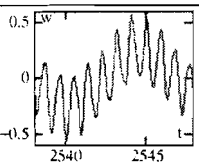	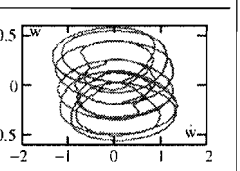

Finally, taking into account the previous description and comments regarding the scenario of transition of our beam into chaotic dynamics monitored via FEM and FDM, the detected scenario fits to the well-known Ruelle-Takens-Newhouse scenario, where in the latter classical case the transition is realized via two independent frequencies and their linear combinations.

References

1. Wang Du, Guo Z, Hagiwara I (2002) Nonlinear vibration control by semi-active piezoactuator damping. JSME Int. J. C. 45(2), 442–448.
2. Awrejcewicz J, Krysko VA (2001) Feigenbaum scenario exhibited by thin plate dynamics. Nonlinear Dynam. 24, 373–398.
3. Awrejcewicz J, Krysko V, Krysko A (2002) Spatial-temporal chaos and solitons exhibited by Von Karman model. Int. J. Bifurcat. Chaos 12(7), 1465–1513.
4. Krysko VA, Shchekutorova TV (2004) Chaotic vibrations of conical shells. Izvestia RAS MTT 4, 140–150 (in Russian).
5. Krysko VA, Zhigalov MV, Saltykova OA, Desatova AS (to appear) Dissipative dynamics of geometrically non-linear Euler-Bernoulli beams. Izvestia RAS MTT.
6. Volmir AS (1972) Nonlinear Dynamics of Plates and Shells. Nauka, Moscow (in Russian).
7. Krysko VA, Awrejcewicz J, Saltykova OA, Chebotyrevskiy YuV (to appear) Nonlinear vibrations of the Euler-Bernoulli beam subject to transversal load and impact actions. Math. Probl. Eng.